Acta Cryst. (1998). A**54**, 1019–1027

Ab Initio Calculation of the Structure Factors and Compton Profiles of Cubic Silicon Carbide

David Ayma,[a]* Michel Rérat,[a] Roberto Orlando[b] and Albert Lichanot[a]

[a]*Laboratoire de Chimie Structurale, UMR 5624, Université de Pau, IFR, rue Jules Ferry, 64000 Pau, France, and* [b]*Dipartimento di Chimica Inorganica, Chimica Fisica e Chimica dei Materiali, Università di Torino, Via P. Giuria 5, 10125 Torino, Italy. E-mail: lichanot@lcshp4.univ-pau.fr*

(*Received 8 December 1997; accepted 1 June 1998*)

Abstract

Crystalline orbitals of cubic silicon carbide have been calculated at the Hartree–Fock and density functional theory (local density approximation) levels using the linear combination of atomic orbitals self-consistent-field method as implemented in the *CRYSTAL*95 code. Charge density, structure factors and Compton profiles are deduced from the crystalline orbitals giving an accurate description of the electronic structure. Thermal motion has been included in the calculations of the charge density and structure factors, and its effect on the charge distribution at room temperature is discussed. The calculated Compton profile and reciprocal-form-factor anisotropies are similar to those characterizing semiconductors of the same family (silicon, diamond and cubic boron nitride) in contrast to previous calculations.

1. Introduction

The numerous and attractive (mechanical, chemical, thermal, electrical and optical) properties of silicon carbide (SiC) explain its growing technological interest particularly for microelectronic devices (Janzèn *et al.*, 1994). SiC crystallizes in either a cubic or a hexagonal structure and forms stable and long-range-ordered modifications, the so-called polytypes (Verma & Krishna, 1966).

First-principles calculations have been applied for determining the electronic band structure of some SiC polytypes (Park *et al.*, 1994; Backes, Bobbert & van Haeringen, 1994; Backes, de Nooij, Bobbert & van Haeringen, 1994; Cubiotti *et al.*, 1997) and its pressure dependence (Aourag *et al.*, 1994; Cheong *et al.*, 1991), pressure-dependent structural properties (Wang *et al.*, 1996), lattice-dynamical properties (Karch *et al.*, 1994, 1995; Karch, Bechstedt *et al.*, 1996*a*,*b*) and thermal properties (Karch, Pavone *et al.*, 1996).

Among about a hundred modifications of SiC, the one with the smallest unit cell, *i.e.* the cubic zinc-blende polytype SiC-3*C* (space group $F\bar{4}3m$) is the most widely investigated. Despite this, SiC-3*C* has not been the subject of intensive theoretical and experimental studies compared to its constituents (diamond and silicon) particularly as regards charge density and its derived properties, structure factors and Compton profiles (CPs). In previous references (Park *et al.*, 1994; Karch *et al.*, 1994, 1995) and in the *ab initio* Hartree–Fock calculations by Orlando *et al.* (1990), charge-density maps reported show unambiguously a large accumulation of charge density around the C atom. According to the Mulliken partition, Orlando *et al.* (1990) report a charge transfer of 1.8 electrons from Si towards C, which is in better agreement with the 'ionic scale' proposed by Christensen *et al.* (1987) than with the one proposed by Phillips (1973). To our knowledge, there is, in contrast to other semiconductors of the same family (silicon, diamond, cubic boron nitride), no recent study of the structure factors and Compton profiles of SiC-3*C* and we must go back to 1982 and 1977 to find experimental (Mahapatra & Padhi, 1979, 1982) and theoretical (Seth & Ellis, 1977) Compton profile values, respectively.

In this work, the *CRYSTAL*95 program (Dovesi *et al.*, 1995) is used to calculate charge density, structure factors, isotropic and directional Compton profiles of SiC-3*C*. The calculations are made both at the Hartree–Fock (HF) and Kohn–Sham (KS) levels where in the latter the exchange and correlation potentials of the electron Hamiltonian are parametrized in the local density approximation (LDA) according to the models of Dirac (1930) and Perdew & Zunger (1981), respectively.

The aim of this work is twofold: (i) to compare the HF and LDA structure factors and Compton profiles in order to evaluate how much of the electron correlation is taken into account by the LDA approach for these properties; (ii) to evaluate thermal corrections of the structure factors and charge density according to the theoretical model developed previously (Azavant *et al.*, 1994, 1996) in order to separate the chemical bonding and temperature effects.

Given that only one set of experimental average Compton profiles (Mahapatra & Padhi, 1979, 1982) and one of theoretical directional Compton profiles (Seth & Ellis, 1977) are available, our calculations are justified particularly in order to check the Compton profile anisotropy calculated by Seth & Ellis, which is surprising

© 1998 International Union of Crystallography
Printed in Great Britain – all rights reserved

ISSN 0108-7673 © 1998

when compared to compounds belonging to the same family (diamond, silicon and cubic boron nitride).

The structure of this paper is the following. A brief description of the computational procedure and of the theoretical background is given in §2. In §3, structural and electronic properties obtained at the HF and LDA levels are reported while in §4 the results of our calculations are discussed and compared with the experiment and other calculations.

2. Computational procedure and theoretical background

2.1. *Computational procedure*

The calculation of the crystalline wave function was performed with the *CRYSTAL*95 code (Dovesi *et al.*, 1995). An exhaustive description of the periodic HF crystalline orbital self-consistent field (SCF) computational scheme embodied in this program is available elsewhere (Pisani *et al.*, 1988), which also contains the Coulomb and exchange series truncation criteria. The Fock matrix has been diagonalized for 29K points of the irreducible part of the first Brillouin zone. All-electron atomic orbital basis sets are adopted to describe the Si and C atoms within the cell. It is of the 8-841G** type for Si with a double set of single Gaussian *d* orbitals (Pisani *et al.*, 1992) and of the 6-21G* type for carbon (Orlando *et al.*, 1990). The exponents of the most diffuse *sp* and *d* shells of each atom have been optimized by searching for the minimum Hartree–Fock crystalline total energy for the experimental lattice parameter. The obtained values are $\alpha_{sp}(\mathrm{Si}) = 0.150$, $\alpha_{sp}(\mathrm{C}) = 0.195$; $\alpha_{1,d}(\mathrm{Si}) = 1.0$, $\alpha_{2,d}(\mathrm{Si}) = 0.3$ and $\alpha_d(\mathrm{C}) = 0.8$. It should be noted that the HF lattice parameter optimized with this basis set is only 0.5% greater than the experimental one (Table 1). However, all the calculations will be performed for the experimental geometry in order to make easier the comparison with our results.

2.2. *Theoretical background*

We recall the main expressions that allow us to calculate the structure factors and Compton profiles in the linear combination of atomic orbitals (LCAO) method. A direct comparison between HF and density functional theory (DFT) methods using the same code, the same basis set and the same computational conditions is possible with *CRYSTAL*95. The HF and KS one-electron equations are solved self-consistently:

$$\hat{H}_{\mathrm{HF/KS}}\varphi^{\mathbf{k}}_{i\,\mathrm{HF/KS}} = \varepsilon^{\mathbf{k}}_{i\,\mathrm{HF/KS}}\varphi^{\mathbf{k}}_{i\,\mathrm{HF/KS}} \tag{1}$$

and the corresponding electron density $\rho(\mathbf{r})$ is calculated:

$$\rho(\mathbf{r}) = \sum_{\mu,\nu,\mathbf{g}} P^{\mathbf{g}}_{\mu\nu}\chi^{\mathbf{0}*}_{\mu}(\mathbf{r})\chi^{\mathbf{g}}_{\nu}(\mathbf{r}), \tag{2}$$

Table 1. *Lattice parameter a (Å), binding energy BE (a.u.) and bulk modulus B (GPa) calculated at the HF and LDA levels*

The HF values of Orlando *et al.* (1990) are given in parentheses and the experimental data are also reported for comparison.

	HF	LDA	Experiment
a	4.382 (4.390)†	4.350	4.360‡
BE	0.35 (0.33)†	0.42	0.48§
B	233 (238)†	224	224‡

† Orlando *et al.* (1990). ‡ Chang & Cohen (1987). § Data from Chang & Cohen (1987) corrected from thermal motion obtained with a Debye temperature $\Theta_D = 1270$ K (Landolt-Börnstein, 1982).

where $\varphi^{\mathbf{k}}_i$ and $\varepsilon^{\mathbf{k}}_i$ are the eigenvectors and eigenvalues, $P^{\mathbf{g}}_{\mu\nu}$ is an element of the density matrix given at the HF or KS level, and $\chi^{\mathbf{0}}_{\mu}$ and $\chi^{\mathbf{g}}_{\nu}$ are the atomic orbitals in the origin (**0**) and **g** cells.

The exchange-correlation potential introduced in the KS one-electron operator is represented as a linear combination of Gaussian-type functions and includes the translational periodicity of the crystal. It is therefore a basis of the total symmetric irreducible representation of the space group. In this work, the KS calculations are performed with the exchange and correlation potentials parametrized in the LDA Dirac (1930) and Perdew–Zunger (1981) models, respectively.

2.2.1. *Structure factors*. Given that the scattering factor in an elastic interaction process is written as

$$f(\mathbf{s}) = \int \rho(\mathbf{r})\exp(-i\mathbf{s}\cdot\mathbf{r})\,\mathrm{d}\mathbf{r}, \tag{3}$$

where $\mathbf{r}$ is the electron position, $\rho(\mathbf{r})$ is the electron density and $\mathbf{s}$ is the scattering vector, $f(\mathbf{s})$ is called the structure factor when expressed in the basis of a crystal cell and is noted as $F_0(\mathbf{s})$ in the static case. The combination of equations (2) and (3) leads to $F_0(\mathbf{s})$, which can be written as (Azavant *et al.*, 1994)

$$F_0(\mathbf{s}) = \sum_{\mu,\nu,\mathbf{g}} P^{\mathbf{g}}_{\mu\nu} I^{g_x}_{0,\mu\nu}(s_x) I^{g_y}_{0,\mu\nu}(s_y) I^{g_z}_{0,\mu\nu}(s_z), \tag{4a}$$

where $I_{0,\mu\nu}$, the static scattering integral, is given by

$$I^{g_x}_{0,\mu\nu}(s_x) = \int\limits_{-\infty}^{+\infty} (x - x_A)^m \exp[-\alpha(x - x_A)^2](x - x_B - g_x)^n \times \exp[-\beta(x - x_B - g_x)^2]\exp(-is_x x)\,\mathrm{d}x. \tag{4b}$$

α and β are the exponents of the Gaussian-type functions (GTFs) associated with the $\mu(A)$ and $\nu(B)$ atomic orbitals (AO) centered on x_A and $x_B + g_x$, respectively, and m and n are dependent on the Gaussian-type orbitals.

In the dynamic case, the structure factor $F_T(\mathbf{s})$ is expressed as formally identical to $F_0(\mathbf{s})$ (Azavant *et al.*, 1994, 1996):

$$F_T(\mathbf{s}) = \sum_{\mu,\nu,\mathbf{g}} P^{\mathbf{g}}_{T,\mu\nu} I^{\mathbf{g}}_{T,\mu\nu}(\mathbf{s}), \tag{5}$$

where the dynamic elements of the density matrix $P^{\mathbf{g}}_{T,\mu\nu}$ take into account the modified overlaps between new α^T and β^T Gaussian functions [see equation (6*c*)].

The expressions for $I^{g_x}_{T,\mu\nu}$ are given by

$$I^{g_x}_{T,\mu\nu}(s_x) = I^{g_x}_{0,\mu\nu}(s_x)\exp(-\tfrac{1}{2}B_{A,xx}s_x^2) \qquad (6a)$$

for pairs of orbitals μ and ν centered on the same atom A with $B_{A,xx}$ the first component of the mean square displacement tensor of the atom A, and

$$I^{g_x}_{T,\mu\nu}(s_x) = (\alpha^T_x/\alpha)^{m+1/2}(\beta^T_x/\beta)^{n+1/2} I^{g_x}_{0,\alpha^T_x\beta^T_x} \qquad (6b)$$

with

$$\alpha^T_x = \alpha/(1+2\alpha B_{A,xx}), \quad \beta^T_x = \beta/(1+2\beta B_{B,xx}) \quad (6c)$$

for pairs of Gaussian (α and β) functions centered on the two atoms A and B localized in the 0 and g_x cells, respectively.

We remind the reader that the model described by equations (5), (6*a*), (6*b*) and (6*c*) is based on three assumptions:

(i) the Debye model is adopted;

(ii) the AOs follow the movements of their associated nuclei;

(iii) the atomic mean square displacement tensors B_{ij} extracted from experimental data are diagonal.

The dynamic elements of the density matrix associated with Gaussian functions described with the new exponents (6*c*) allow us to calculate the corresponding electron density and to draw dynamic electron charge density maps, thanks to a subroutine introduced in the *CRYSTAL* code.

2.2.2. *Compton profiles*. In the high-energy inelastic scattering of photons by electrons and within the impulse approximation (Cooper, 1985), the Compton profile $J(q)$ is defined as the projection of the electron momentum distribution (EMD) $\rho(p)$ along the scattering vector (s_z) for a given value of the momentum ($p_z = q$):

$$J(q) = \int_{p_x p_y} \rho(\mathbf{p})\,\mathrm{d}p_x\,\mathrm{d}p_y. \qquad (7)$$

In momentum space, expression (2) becomes

$$\rho(\mathbf{p}) = \sum_{\mu,\nu,\mathbf{g}} P^{\mathbf{g}}_{\mu\nu}\chi^{\mathbf{0}*}_{\mu}(\mathbf{p})\chi^{\mathbf{g}}_{\nu}(\mathbf{p}), \qquad (8)$$

where $\chi^{\mathbf{0}*}_{\mu}(\mathbf{p})$ and $\chi^{\mathbf{g}}_{\nu}(\mathbf{p})$ are the Fourier transformations of $\chi^{\mathbf{0}}_{\mu}(\mathbf{r})$ and $\chi^{\mathbf{g}}_{\nu}(\mathbf{r})$:

$$\chi(\mathbf{p}) = \int \chi(\mathbf{r})\exp(-i\mathbf{p}\cdot\mathbf{r})\,\mathrm{d}\mathbf{r}. \qquad (9)$$

Finally, the directional Compton profile expression is written as

$$J(q) = \sum_{\mu,\nu,\mathbf{g}} P^{\mathbf{g}}_{\mu\nu} \int_{p_x p_y} \chi^{\mathbf{0}*}_{\mu}(\mathbf{p})\chi^{\mathbf{g}}_{\nu}(\mathbf{p})\,\mathrm{d}p_x\,\mathrm{d}p_y. \qquad (10)$$

These integrals can be calculated analytically (Appendix *A* in Rérat & Lichanot, 1997).

The isotropic Compton profile can also be calculated numerically as the average value over all the directions with the following expression:

$$\bar{J}(q) = \int_{p=q}^{\infty} \bar{\rho}(\mathbf{p}) 2\pi p\,\mathrm{d}p. \qquad (11)$$

In order to obtain the average Compton profile, we firstly integrate analytically the electronic density $\bar{\rho}(\mathbf{p})$ according to

$$\bar{\rho}(\mathbf{p}) = \sum_{\mu,\nu,\mathbf{g}} P^{\mathbf{g}}_{\mu\nu}(1/4\pi)\int_{\theta=0}^{\pi}\int_{\varphi=0}^{2\pi} \chi^{\mathbf{0}*}_{\mu}(\mathbf{p})\chi^{\mathbf{g}}_{\nu}(\mathbf{p})\sin\theta\,\mathrm{d}\theta\,\mathrm{d}\varphi \qquad (12)$$

over the spherical (θ, φ) coordinates corresponding to the p_z direction.

3. Results

Before reporting the calculations of the charge density, structure factors and Compton profiles of SiC-3*C*, HF physical properties depending on the total energy (lattice parameter, binding energy and bulk modulus) calculated with the new basis set are compared with the values already obtained by Orlando *et al.* (1990) using a 6-21G* basis set for the two atoms. Table 1 shows that: (i) the use of the 8-841G** basis set for Si instead of the 6-21G* set improves slightly the results of Orlando *et al.* (1990) but the HF lattice parameter and bulk modulus are always overestimated with respect to experiment; (ii) the use of DFT at the LDA level leads to very satisfactory values since the lattice parameter is underestimated (as expected) by only 0.3% and the bulk modulus is exactly reproduced. However, the binding energy in LDA, which approximately takes into account electron correlation, is still 12% smaller than the experimental value.

3.1. *Charge density and structure factors*

In order to be able to compare our results directly with experiment, the following calculations have been made in the experimental geometry. The electronic structure of SiC-3*C* is represented by the electron charge density (ECHD) maps through the (110) plane (Fig. 1). For reasons of clarity, we limit ourselves to three representations which allow us to discuss the bonding, electron correlation and temperature effects, respectively. Fig. 1(*a*) gives the static difference ECHD at the LDA level between the bulk and the superposition of independent atoms described with the same basis set as used in the bulk. It shows a large build-up of electron charge along the Si-C bond, which is slightly shifted towards the carbon atom. This supports the idea that the chemical bond in SiC-3*C* is mainly covalent but is slightly disturbed by an electron charge transfer from silicon to carbon (semi-covalent bond). Fig. 1(*b*)

presents the difference between the bulk ECHD maps obtained with the LDA and HF approaches. Along the SiC direction, the difference LDA − HF charge density is very small and alternately positive, negative, positive from one nucleus to the other. Close to the middle of the bond where most of the bond charge is concentrated, there is a deficiency of charge in the LDA approach. On the contrary, a positive difference is observed in the nonbonding directions around the Si atoms showing a larger overlap population between the Si second neighbors in the LDA level. Finally, Fig. 1(*c*) reports the difference between the dynamic ($T = 298$ K) and the static bulk ECHD maps obtained at the LDA level. In the dynamic case, the elements of the density matrix [equation (6*a*)] are calculated at $T = 298$ K by adopting for the Debye–Waller factors $B_{\rm Si} = 0.55$, $B_{\rm C} = 0.67$ Å^2 deduced from the atomic mean square displacements given by Vetelino *et al.* (1972). The concentration of negative isodensity curves around carbon shows that the charge transfer from Si to C becomes smaller at $T = 298$ K and that the covalent part of the SiC bond is slightly increased. On the other hand, the regular shape of the consecutive isodensity curves indicates also that the chemical (static) deformation of the electron clouds

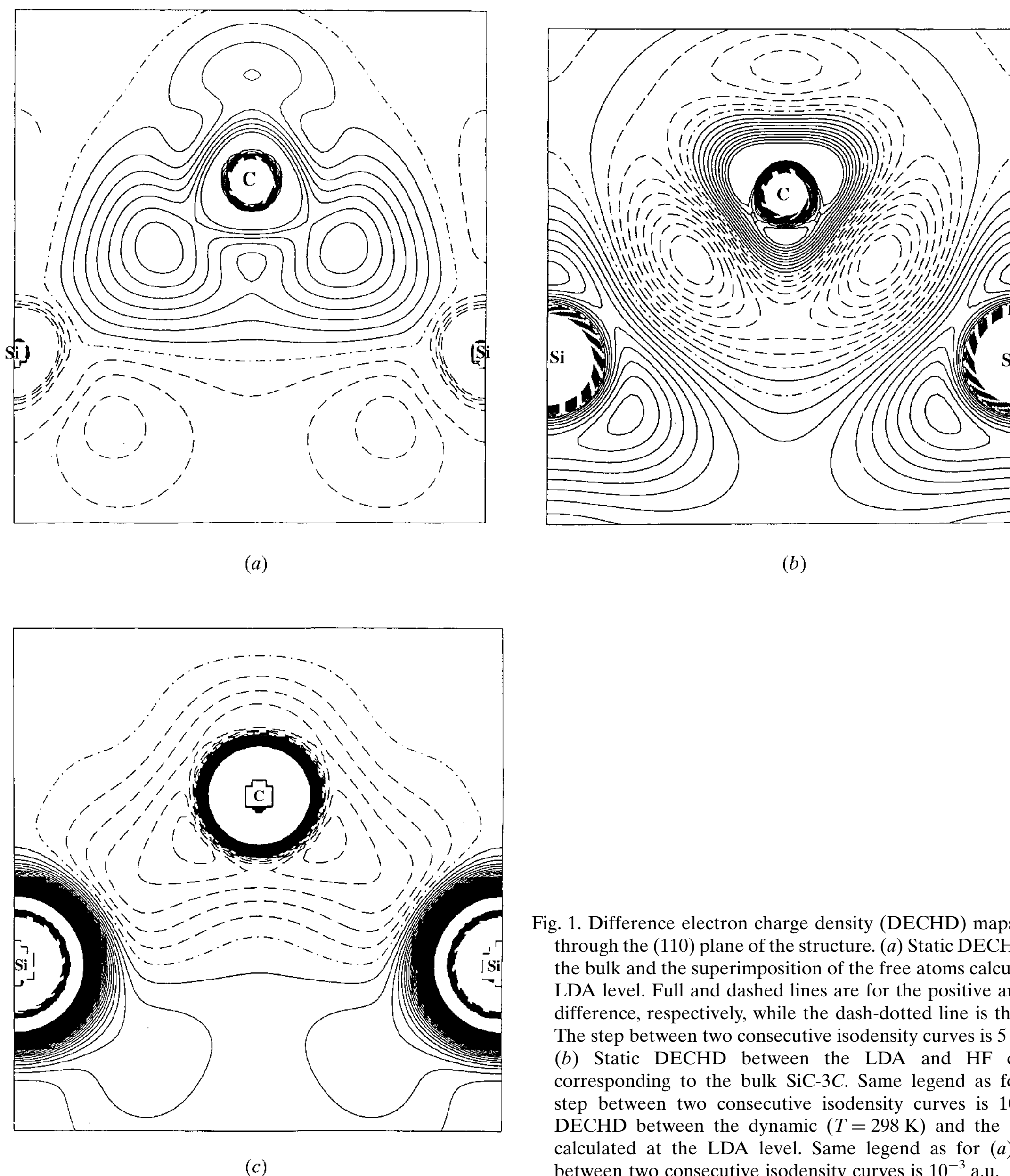

Fig. 1. Difference electron charge density (DECHD) maps of SiC-3*C* through the (110) plane of the structure. (*a*) Static DECHD between the bulk and the superimposition of the free atoms calculated at the LDA level. Full and dashed lines are for the positive and negative difference, respectively, while the dash-dotted line is the zero line. The step between two consecutive isodensity curves is 5×10^{-3} a.u. (*b*) Static DECHD between the LDA and HF calculations corresponding to the bulk SiC-3*C*. Same legend as for (*a*). The step between two consecutive isodensity curves is 10^{-3} a.u. (*c*) DECHD between the dynamic ($T = 298$ K) and the static cases calculated at the LDA level. Same legend as for (*a*). The step between two consecutive isodensity curves is 10^{-3} a.u.

is practically not altered at this temperature by the thermal motion.

The same kind of observations can be carried out from the results of the structure factors given in Table 2 and Fig. 2. The static and dynamic ($T = 298$ K) structure factors given in Table 2 have been calculated from expressions (4*a*), (4*b*) and (5), respectively, for all the reflections with $(\sin\theta)/\lambda < 1\ \text{Å}^{-1}$. In the absence of recent and accurate X-ray experimental data, the dynamic structure factors have been calculated with two sets of Debye–Waller factors known at $T = 298$ K. The first one is given by Reid (1983) ($B_{\rm Si} = 0.218$, $B_{\rm C} = 0.226\ \text{Å}^2$) whereas the second one is deduced from a temperature-dependent study of the Debye–Waller factor for zinc-blende-type crystals by Vetelino *et al.* (1972) ($B_{\rm Si} = 0.55$, $B_{\rm C} = 0.67\ \text{Å}^2$). These last values will be preferred for the following discussion for two reasons. (i) The Si and C atoms are on sites of the same symmetry ($\bar{4}3m$) and the magnitude of the C displacement, greater than the Si one at room temperature, is better described by the values of Vetelino *et al.* (ii) They are also in better agreement with those coming from other studies, *e.g.* that of Inagaki *et al.* (1987), which determines the effective Debye–Waller parameter from the plots of integrated intensity of X-ray diffraction lines against $(\sin\theta/\lambda)^2$, and that of Karch *et al.* (1995), which deduces the mean square atomic displacements from *ab initio* calculation of lattice dynamical properties. To discuss the deformation of the electron clouds around the atoms, it is convenient to compare the F_0 values (column 3 of Table 2) with those calculated in the independent-atom model (IAM) in which the crystal is represented by a superposition of free atoms. For the zinc-blende-type structure, the expressions for the $F_0^{\rm IAM}$ are given by

$$F_0^{\rm IAM} = \begin{cases} 4[f_{0,{\rm Si}} + f_{0,{\rm C}}] & \text{for } h+k+l = 4n \\ 4[f_{0,{\rm Si}} + if_{0,{\rm C}}] & \text{for } h+k+l = 4n+1 \\ 4[f_{0,{\rm Si}} - f_{0,{\rm C}}] & \text{for } h+k+l = 4n+2 \\ 4[f_{0,{\rm Si}} - if_{0,{\rm C}}] & \text{for } h+k+l = 4n-1. \end{cases}$$

$F_0^{\rm IAM}$ is calculated using for the atomic scattering factors f_0 both the values given in *International Tables for Crystallography* (1992) and also those values deduced from the wave function of the free atoms described with the same basis set as for the bulk. The corresponding differences $\Delta F_0 = F_0 - F_0^{\rm IAM}$ are represented by symbols ● and □, respectively, and are shown *versus* $(\sin\theta)/\lambda$ in Fig. 2. The closeness of the symbols ● and □ for each $(\sin\theta)/\lambda$ value indicates that the AO basis sets describing the free atoms in this work and *International Tables for Crystallography* are of comparable quality. These differences (with respect to the zero line) show significant deviations only for the first six reflections especially for the 111 and 200. The largest positive difference associated with the 111 reflection contains the contributions from both Si and C atoms and expresses the deformation of their electron clouds along the [111] direction. It is correlated in part to the covalent character of the Si—C bond. The negative difference asso-

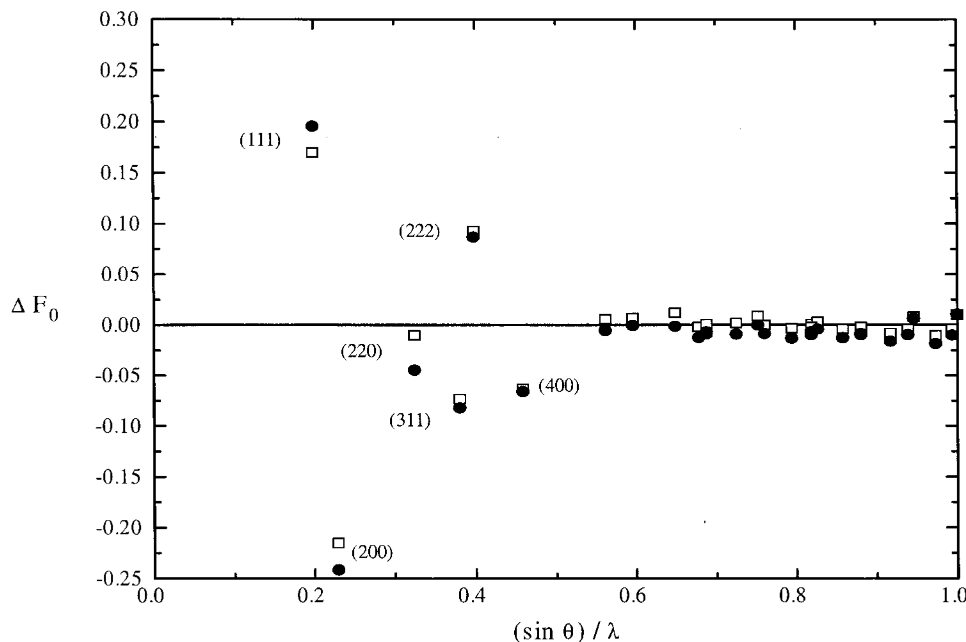

Fig. 2. Static difference between the structure factors of SiC-3*C* (column 3 of Table 2) and $F_0^{\rm IAM}$. Symbols ● and □ are for $F_0^{\rm IAM}$ calculated from *International Tables for Crystallography* (1992) and for $F_0^{\rm IAM}$ calculated with the basis sets used for the bulk, respectively.

Table 2. *Static (F_0) and dynamic (F_T) structure factors corresponding to the unit cell, calculated at the LDA level*

$F_T(a)$ and $F_T(b)$ are calculated with the pairs $B_{\rm Si} = 0.55$, $B_{\rm C} = 0.67$ Å^2 (Vetelino *et al.*, 1972) and $B_{\rm Si} = 0.218$, $B_{\rm C} = 0.226$ Å^2 (Reid, 1983), respectively.

hkl	$(\sin\theta)/\lambda$ (Å^{-1})	F_0	$F_T(a)$	$F_T(b)$
1 1 1	0.1986	10.540	10.303	10.436
2 0 0	0.2294	5.759	5.618	5.694
2 2 0	0.3244	10.250	9.636	10.011
2 2 2	0.3973	5.288	4.889	5.114
3 1 1	0.3803	7.571	6.978	7.336
3 3 1	0.4999	6.481	5.639	6.136
3 3 3	0.5959	5.515	4.522	5.103
4 0 0	0.4587	8.325	7.370	7.949
4 2 0	0.5129	4.454	3.903	4.211
4 2 2	0.5618	7.213	6.013	6.729
4 4 0	0.6487	6.342	4.974	5.782
4 4 2	0.6880	3.105	2.457	2.807
4 4 4	0.7945	5.084	3.525	4.424
5 1 1	0.5959	5.542	4.545	5.128
5 3 1	0.6784	4.833	3.736	4.371
5 3 3	0.7520	4.284	3.119	3.785
5 5 1	0.8190	3.833	2.629	3.310
5 5 3	0.8809	3.469	2.241	2.928
5 5 5	0.9931	2.930	1.678	2.361
6 0 0	0.6880	3.107	2.459	2.809
6 2 0	0.7253	5.643	4.162	5.027
6 2 2	0.7607	2.638	1.987	2.332
6 4 0	0.8270	2.274	1.632	1.966
6 4 2	0.8582	4.622	3.013	3.931
6 4 4	0.9457	1.768	1.154	1.462
6 6 0	0.9731	3.923	2.259	3.185
6 6 2	0.9997	1.593	0.991	1.288
7 1 1	0.8190	3.831	2.628	3.308
7 3 1	0.8809	3.470	2.241	2.928
7 3 3	0.9387	3.174	1.931	2.617
7 5 1	0.9931	2.930	1.678	2.361
8 0 0	0.9174	4.241	2.598	3.524
8 2 0	0.9457	1.768	1.154	1.462
8 2 2	0.9731	3.923	2.259	3.185

ciated with the 200 reflection can be attributed to the charge transfer between Si and C [this difference is null in the silicon crystal (Pisani *et al.*, 1992)] whereas the 222 reflection describes again the charge transfer but also the asphericity of the charge density. Finally, we note that the HF structure factors (not reported in Table 2 for reasons of clarity) are very close to the LDA ones. The HF values are always slightly smaller by about 0.4% than the LDA ones. Only three reflections make an exception to this rule; the 222 reflection for which the difference LDA − HF structure factors reaches 1.3%, and the 200 and 220 reflections for which the difference is negative but remains very small. We remark that these three reflections are closely related to the charge transfer between Si and C which is different by about 0.5 electrons between the LDA and HF approaches (see §4). Generally speaking, these results indicate that the part of the electron correlation included in the LDA approach has a rather small but significant effect on the reflections that are sensitive to the bonding. It should be noted that such a result has also been shown in silicon where the experimental and theoretical charge densities are accurately compared (Zuo *et al.*, 1997). In this study, it is also shown that the gradient corrected DFT sheme is of better quality than the LDA–DFT one to describe the distribution of the valence electrons.

3.2. *Compton profiles*

Static average total (normalized to the 20 electrons of the unit cell) and directional valence (normalized to 8 electrons) Compton profiles are given in Table 3. Given the fact that in momentum space the Compton profiles cannot be directly deduced from the KS wavefunctions (Weyrich, 1996), only the HF calculations are reported in this table. Our theoretical values $J_{\rm tot}$ are also given (in parentheses) when convoluted with a residual instrumental function (RIF = 0.57 a.u.) in order to facilitate a comparison with the experimental data of Mahapatra & Padhi (1979, 1982). Preliminary observations can be deduced from our results.

(i) Our theoretical values are smaller than the experimental ones at the smallest q values ($q < 1.0$ a.u.). The agreement factor defined as

$$R = \sum_q |J_{\rm calc} - J_{\rm exp}| \Big/ \sum_q J_{\rm exp},$$

where $J_{\rm calc}$ and $J_{\rm exp}$ are our HF and experimental Compton profiles, respectively, is only 4.5%, a value that is higher than those recently obtained for other compounds of the same family ($R = 3\%$ for diamond, $R = 4\%$ for cubic BN) (Ayma *et al.*, 1998).

(ii) In order to continue the comparison of our values with those in the literature, the Compton profile anisotropies ($J_{100} - J_{110}$) and ($J_{100} - J_{111}$) are calculated and they are shown in Fig. 3 together with the calculation of Seth & Ellis (1977) who used a Slater-type orbital basis set. The agreement is satisfactory for the $\Delta J(q) = J_{100} - J_{110}$ curve, for which the shape and height of the peaks are well described. On the contrary, the discrepancy observed for the $\Delta J(q) = J_{100} - J_{111}$ curve is significant except that a shoulder in the curve is obtained for a value of q around 0.9 a.u. in both cases. A second basis set (6-21G* for the two atoms) of poorer quality was used but the results are close to the ones obtained with the 8-841G** basis set and thus did not improve with respect to the calculations of Seth & Ellis (1977).

4. Discussion

With respect to the two reference compounds of the same family, namely silicon and diamond, the substitution of one Si (or C) by one C (or Si) in the unit cell changes the space-group symmetry of the conventional cell from the centrosymmetric *Fd*3*m* to the noncen-

trosymmetric $F\bar{4}3m$ group for SiC. As a consequence, the purely covalent character of silicon is modified into a semicovalent one in the case of SiC-3*C*. The main features that demonstrate this character are summarized next. In silicon, the difference (bulk minus atomic superposition) charge-density maps show a high diffuse bond charge centered at the midpoint of the Si—Si bond (Pisani *et al.*, 1992). The electron distribution around the Si atoms is aspherical since the 'forbidden' 222 reflection has a structure factor $F_{222} = 0.217$. In SiC-3*C*, the bond charge is disturbed by an electron charge transfer from Si to C and the saddle point of the difference ECHD is localized closer to the carbon site. The disturbance of the valence-electron cloud along the [111] direction shows up in the large positive value of the difference $F_{111} - F_{111}^{\rm IAM}$ while the charge transfer from Si to C corresponds to the value of the difference in the structure factors associated with the 200 reflection

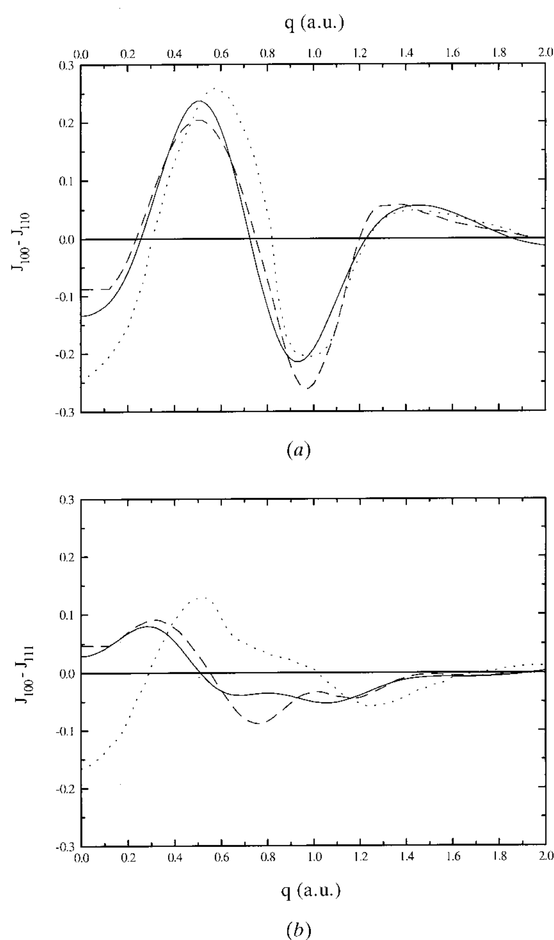

Fig. 3. Valence Compton profile anisotropy $\Delta J(q)$ calculated at the HF level. (*a*) $\Delta J(q) = J_{100}(q) - J_{110}(q)$. (*b*) $\Delta J(q) = J_{100}(q) - J_{111}(q)$. Full and dashed lines correspond to our calculations using for silicon the 8-841G** and 6-21G* basis sets, respectively. Dotted lines correspond to the calculations of Seth & Ellis (1977).

Table 3. *Static average total J_{tot} and directional valence J_{val} Compton profiles calculated at the HF level*

The values in parentheses correspond to the theoretical ones convoluted by a RIF = 0.57 a.u. (Mahapatra & Padhi, 1979, 1982).

q	$J_{\rm exp}$†	$J_{\rm tot}$	$J_{\rm val}(100)$	$J_{\rm val}(110)$	$J_{\rm val}(111)$
0.0	6.434	6.321 (6.125)	4.307	4.441	4.278
0.1	6.399	6.289 (6.093)	4.308	4.427	4.267
0.2	6.298	6.190 (5.996)	4.291	4.350	4.223
0.3	6.128	6.026 (5.836)	4.205	4.152	4.126
0.4	5.890	5.799 (5.614)	4.016	3.841	3.963
0.5	5.585	5.508 (5.334)	3.729	3.492	3.724
0.6	5.218	5.157 (5.001)	3.363	3.175	3.395
0.7	4.798	4.749 (4.623)	2.932	2.889	2.971
0.8	4.338	4.290 (4.213)	2.444	2.563	2.479
0.9	3.858	3.794 (3.787)	1.927	2.137	1.968
1.0	3.380	3.273 (3.366)	1.437	1.629	1.488
1.2	2.523	2.392 (2.615)	0.724	0.744	0.763
1.4	1.909	1.895 (2.069)	0.386	0.332	0.398
1.6	1.558	1.643 (1.722)	0.243	0.199	0.250
1.8	1.380	1.472 (1.501)	0.172	0.164	0.178
2.0	1.260	1.327 (1.340)	0.132	0.145	0.128
2.5	0.957	1.018 (1.027)	0.076	0.069	0.057
3.0	0.737	0.782 (0.788)	0.045	0.047	0.043
3.5	0.568	0.598 (0.604)	0.029	0.029	0.037
4.0	0.435	0.459 (0.463)	0.019	0.019	0.021
5.0	0.269	0.280 (0.282)	0.009	0.009	0.009
6.0	0.183	0.180 (0.181)	0.005	0.005	0.005
7.0	0.139	0.122 (0.123)	0.003	0.003	0.003

† Mahapatra & Padhi (1979, 1982).

$F_{200} - F_{200}^{\rm IAM}$. These data are confirmed by a Mulliken population analysis since, in LDA, the total charges of the Si and C atoms are 13.02 and 6.98 electrons, respectively, indicating a charge transfer of 0.98 electrons. The overlap population between the first-nearest neighbors is 0.32 electrons. It should be noted that at the HF level the character of SiC-3*C* is more ionic since the charge transfer is higher (1.45 electrons) while the overlap population is not modified (0.33 electrons). Finally, the electronic structure of SiC-3*C* is rather close to that of the cubic BN recently studied with the HF approach by Lichanot *et al.* (1996). In fact, this compound belonging to the III–V semiconductor family with the same zinc-blende-type structure has the same characteristics as SiC-3*C*. However, its covalent character is greater than SiC-3*C* owing to a smaller charge transfer (0.8 electrons) from boron to nitrogen and a higher overlap population (0.5 electrons) between the B and N atoms.

In §3.2, we have underlined the discrepancy observed between our calculations of the Compton profile anisotropy $J_{100} - J_{111}$ and those of Seth & Ellis (1977). This discrepancy probably stems from the calculation of the Compton profile along the bond direction [111], since the results of the $J_{100} - J_{110}$ anisotropy are in satisfactory agreement. Without experimental data and other calculations to confirm these results, it seems however that our calculations lead to a situation more realistic than that of Seth & Ellis (1977) for the following

reason. If we consider the homogeneous family of the IV and III—V semiconductors with the zinc-blende-type structure, we notice that in all cases the $J_{100} - J_{111}$ anisotropy of diamond (Dovesi *et al.*, 1981; Wepfer *et al.*, 1974; Euwema *et al.*, 1974; Ayma *et al.*, 1998; Reed & Eisenberger, 1972; Weiss & Phillips, 1968; Seth & Ellis, 1977; Schülke & Kramers, 1979), silicon (Pisani *et al.*, 1992; Reed & Eisenberger, 1972; Pattison *et al.*, 1981; Schülke & Kramers, 1979) and cubic boron nitride (Ayma *et al.*, 1998; Dovesi *et al.*, 1981) is positive for the smallest values of the momentum (q). Our calculations (Fig. 2) show the same result for SiC-3*C* while the $J_{100} - J_{111}$ anisotropy obtained by Seth & Ellis (1977) is very negative. It should be remarked that the Bloch functions calculated by Seth & Ellis are generated from Slater-type orbitals (STO). It seems likely that the STO Si basis used by these authors is of poorer quality than the C one since the agreement of the Compton profiles is less for silicon than for diamond. This effect seems amplified in SiC-3*C* with the more ionic character of this compound. At this stage of the comparison, it should be noted that the observed $J_{100} - J_{111}$ anisotropy shows the sequence C > Si > *c*-BN > SiC-3*C* and thus follows partly the increase in charge transfer between the two atoms of the bond; the higher the charge transfer, the smaller the $J_{100} - J_{111}$ Compton profile anisotropy. Of course, other features such as the interatomic distance, number of shells around the atoms and polarizability of the electron clouds are also parameters to be considered to explain this sequence. Work in this direction is in progress.

In order to make the identification of bonding features in Compton profiles easier, it is natural to return to the direct space by introducing the reciprocal form factor or autocorrelation function $B(\mathbf{r})$ as the Fourier transformation of the Compton profile. Thus, the one-dimensional Fourier transformation

$$B(z) = \int J(q = p_z) \exp(-ip_z z) \, \mathrm{d}p_z$$

has been calculated along the three principal directions and the reciprocal-form-factor anisotropies are reported in Fig. 4. Before discussing the $B(\mathbf{r})$ anisotropy, it should be noted that the $B(z)$ curves associated with the [100] and [110] directions cross the z axis at the values 4.37 and 3.09 Å, which correspond to the lattice parameters a and $a/2^{1/2}$, respectively. This result, valid for insulators and semiconductors with filled bands, provides thus a valuable check on the accuracy and reliability of the calculated wave functions. The $B_{100} - B_{111}$ and $B_{100} - B_{110}$ differences (Fig. 4) reveal strong effects of the bond anisotropy and the antibonding interactions, respectively, under the assumption that the [100] direction acts as a neutral direction (Pattison *et al.*, 1981). The $B_{100} - B_{111}$ anisotropy shows a large peak at the distance $z = a \times 3^{1/2}/4$ between the nearest neighbors and the height of the maximum of the curve is smaller than that observed in *c*-BN and diamond. The maximum anisotropy along the [110] direction takes place for $z = a/2^{1/2}$ and indicates a nonbonding interaction between the orbitals associated with the second-nearest neighbors. The diffuse character of the bond charge shown in the difference ECHD maps of Fig. 1(*a*) makes this last interaction rather easy.

5. Conclusions

The electronic structure of SiC-3*C* has been theoretically obtained from the charge density, structure factors (calculated in the LDA and HF-LCAO models) and HF Compton profiles where both atoms are described with all-electron basis sets. The difference electron charge-density maps and the analysis of the structure factors associated with the 111 and 200 reflections show that the chemical bond in SiC-3*C* is semicovalent with a significant charge transfer from silicon to carbon.

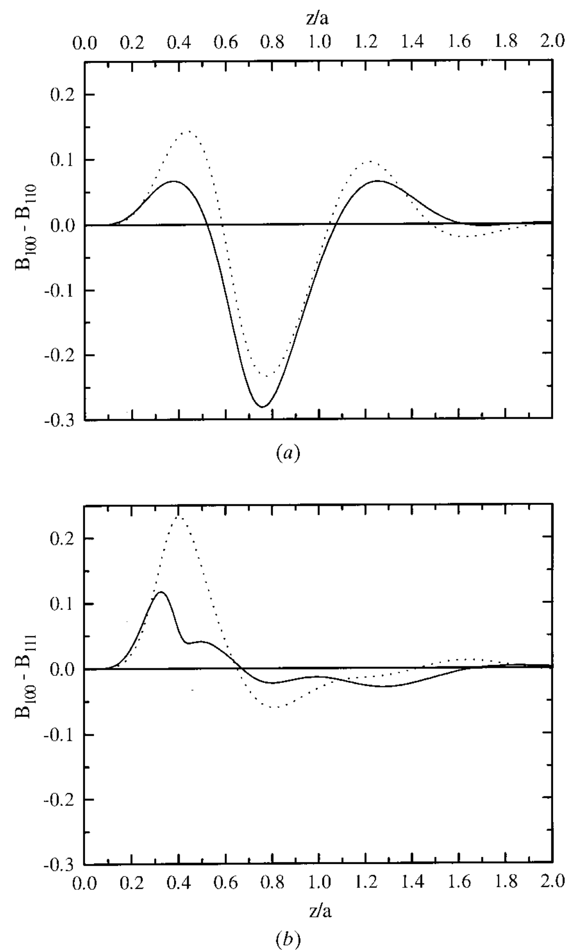

Fig. 4. Reciprocal form factor anisotropy $\Delta B(r)$ calculated at the HF level. (*a*) $\Delta B(r) = B_{100} - B_{110}$. (*b*) $\Delta B(r) = B_{100} - B_{111}$. Full lines are for SiC-3*C* while dotted ones are for *c*-BN (Ayma *et al.*, 1998).

Averaged and directional Compton profiles and the related functions such as the reciprocal form factors have been analyzed. They show a behavior similar to other compounds of the same family, namely diamond, silicon and cubic boron nitride. This result is in contrast to earlier calculations of Seth & Ellis (1977) which have shown a negative Compton profile anisotropy in the bond direction. However, it would be interesting to confirm our calculations by other theoretical approaches but even better by accurate measurement of average and directional Compton profiles. Electron correlation effects approximately included in the LDA approach for calculating structure factors and charge densities are rather small but significant. However, insufficient experimental data do not allow us to conclude whether or not correlation effects are large.

Finally, a detailed comparison of these properties for similar compounds is desirable to separate the effects of the intra-atomic distance from the valence-electron configuration.

References

Aourag, H., Djelouli, B., Hazzab, A. & Khelifa, B. (1994). *Mater. Chem. Phys.* **39**, 34–39.

Ayma, D., Rérat, M. & Lichanot, A. (1998). *J. Phys. Condens. Matter*, **10**, 557.

Azavant, P., Lichanot, A., Rérat, M. & Chaillet, M. (1994). *Theor. Chim. Acta*, **89**, 213–226.

Azavant, P., Lichanot, A., Rérat, M. & Pisani, C. (1996). *Int. J. Quantum Chem.* **58**, 419–429.

Backes, W. H., Bobbert, P. A. & van Haeringen, W. (1994). *Phys. Rev. B*, **49**, 7564–7568.

Backes, W. H., de Nooij, F. C., Bobbert, P. A. & van Haeringen, W. (1994). *Physica (Utrecht)*, B**217**, 207–211.

Chang, K. J. & Cohen, M. L. (1987). *Phys. Rev. B*, **35**, 8196–8201.

Cheong, B. H., Chang, K. J. & Cohen, M. L. (1991). *Phys. Rev. B*, **44**, 1053–1056.

Christensen, N. E., Satpathy, S. & Pawlowska, Z. (1987). *Phys. Rev. B*, **36**, 1032–1036.

Cooper, M. J. (1985). *Rep. Prog. Phys.* **48**, 415–481.

Cubiotti, G., Kucherenko, Y. N. & Antonov, V. N. (1997). *J. Phys. Condens. Matter*, **9**, 165–175.

Dirac, P. A. M. (1930). *Proc. Cambridge Philos. Soc.* **26**, 376–380.

Dovesi, R., Pisani, C., Roetti, C. & Dellarole, P. (1981). *Phys. Rev. B*, **24**, 4170–4176.

Dovesi, R., Saunders, V. R., Roetti, C., Causà, M., Harrison, N. M., Orlando, R. & Aprà, E. (1995). *CRYSTAL95 Users Manual.* Theoretical Chemistry Group, Turin, Italy, and CCLRC Daresbury Laboratory, England.

Euwema, R. N., Surrat, G. T., Wilhite, D. L. & Wepfer, G. G. (1974). *Philos. Mag.* **29**, 1033–1039.

Inagaki, M., Toyoda, M. & Sakai, M. (1987). *J. Mater. Sci.* **22**, 3459–3462.

International Tables for Crystallography (1992). Vol. A. Dordrecht: Kluwer Academic Publishers.

Janzèn, E., Kordina, O., Henry, A., Chen, W. M., Son, N. T., Monemar, B., Sörman, E., Bergman, P., Harris, C. I., Yakimova, R., Tuominen, M., Konstantinov, A. O., Hallin, C. & Hemmingsson, C. (1994). *Phys. Scr.* **154**, 283–290.

Karch, K., Bechstedt, F., Pavone, P. & Strauch, D. (1996*a*). *J. Phys. Condens. Matter*, **8**, 2945–2955.

Karch, K., Bechstedt, F., Pavone, P. & Strauch, D. (1996*b*). *Phys. Rev. B*, **53**, 13400–13413.

Karch, K., Pavone, P., Mayer, A. P., Bechstedt, F. & Strauch, D. (1996). *Physica (Utrecht)*, B**219**, 448–450.

Karch, K., Pavone, P., Windl, W., Schütt, O. & Strauch, D. (1994). *Phys. Rev. B*, **50**, 17054–17063.

Karch, K., Pavone, P., Windl, W., Strauch, D. & Bechstedt, F. (1995). *Int. J. Quantum Chem.* **56**, 801–817.

Landolt-Börnstein (1982). New Series, Vol. 17*a*, edited by O. Madelung. Berlin: Springer.

Lichanot, A., Azavant, P. & Pietsch, U. (1996). *Acta Cryst.* B**52**, 586–595.

Mahapatra, D. P. & Padhi, H. C. (1979). *Nucl. Phys. Solid State Phys. India*, **22**C, 70–73.

Mahapatra, D. P. & Padhi, H. C. (1982). *Philos. Mag.* B**46**, 607–610.

Orlando, R., Dovesi, R., Roetti, C. & Saunders, V. R. (1990). *J. Phys. Condens. Matter*, **2**, 7769–7789.

Park, C. H., Cheong, B. H., Lee, K. H. & Chang, K. J. (1994). *Phys. Rev. B*, **49**, 4485–4493.

Pattison, P., Hansen, N. K. & Schneider, J. R. (1981). *Chem. Phys.* **59**, 231–242.

Perdew, J. P. & Zunger, A. (1981). *Phys. Rev. B*, **23**, 5048–5050.

Phillips, J. C. (1973). *Bonds and Bands in Semiconductors.* New York: Academic Press.

Pisani, C., Dovesi, R. & Orlando, R. (1992). *Int. J. Quantum Chem.* **42**, 5–33.

Pisani, C., Dovesi, R. & Roetti, C. (1988). *Hartree–Fock Ab Initio Treatment of Crystalline Systems. Lecture Notes in Chemistry*, Vol. 48. Heidelberg: Springer.

Reed, W. A. & Eisenberger, P. (1972). *Phys. Rev. B*, **6**, 4596–4604.

Reid, J. S. (1983). *Acta Cryst.* A**39**, 1–13.

Rérat, M. & Lichanot, A. (1997). *Chem. Phys. Lett.* **263**, 767–774.

Schülke, W. & Kramers, B. (1979). *Acta Cryst.* A**35**, 953–957.

Seth, A. & Ellis, D. E. (1977). *J. Phys. C*, **10**, 181–194.

Verma, A. R. & Krishna, P. (1966). *Polymorphism and Polytypism in Crystals.* New York: Wiley.

Vetelino, J. F., Gaur, S. P. & Mitra, S. S. (1972). *Phys. Rev. B*, **5**, 2360–2366.

Wang, C. Z., Yu, R. & Krakauer, H. (1996). *Phys. Rev. B*, **53**, 5430–5437.

Weiss, R. J. & Phillips, W. C. (1968). *Phys. Rev.* **176**, 900–904.

Wepfer, G. G., Euwema, R. N., Surrat, G. T. & Wilhite, D. L. (1974). *Phys. Rev. B*, **9**, 2670–2673.

Weyrich, W. (1996). *Quantum-Mechanical Ab Initio Calculation of the Properties of Crystalline Materials*, edited by C. Pisani. *Lecture Notes in Chemistry*, Vol. 67. Heidelberg: Springer.

Zuo, J. M., Blaha, P. & Schwarz, K. (1997). *J. Phys. Condens. Matter*, **9**, 7541–7561.